

Decreasing the number of test specimens by utilizing both fracture stress and fracture location for the estimation of Weibull parameter

Y. MATSUO

Department of Metallurgy & Ceramic Science, Tokyo Institute of Technology, Meguro-ku, Tokyo 152-8552, Japan

T. NAKAMOTO

Fuji Xerox Co., Ltd., Quality Assurance and Management Ebina 239-0494, Japan

K. SUZUKI, W. YAMAMOTO

Department of Systems Engineering, The University of Electro-Communications, Chofu-City, Tokyo 182-8585, Japan

E-mail: suzuki@se.uec.ac.jp

In a bending load test for brittle materials, such as ceramics for spacecraft and aircraft, decreasing the number of test specimens required is a crucial problem. This paper discusses the effectiveness of using the information of both fracture stress and fracture location to decrease the number of specimens required to obtain the same precision as the Weibull estimator. The following results were obtained: It was found that by adding the fracture location information, the precision of the Weibull parameter estimation under the optimal design became 1.5–1.9 times better compared with the case of using only the fracture stresses. This means the number of samples necessary to attain the same precision becomes 1/1.5–1/1.9. Tables and figures which give information on the number of samples necessary to attain the required precision are given. © 2004 Kluwer Academic Publishers

1. Introduction

Brittle materials such as ceramics have not been frequently used as structural materials because of their low reliability. In recent years, however, structural ceramics have been viewed with increasing interest because of the rapid progress in the improvement of their mechanical and physicochemical properties. Since almost all structural ceramics fail in a brittle manner, they tend to have a wide strength scatter. Therefore, implementing a loading test on nominally identical specimens and obtaining a distribution of strength are becoming important. Hence, the weakest link theory by Weibull [1] has been playing important roles.

Oh and Finnie [2] developed a statistical theory of fracture location which can be used to estimate not only the fracture stress but also the fracture location using Weibull's function. Aoki and Sakata [3] and Aoki *et al.* [4] applied this theory on brittle fracture and proved its validity. Matsuo and Kitakami [5, 6] combined the statistical theory of fracture location with a competing risk theory since ceramics may contain many kinds of defects.

The number of test specimens in a loading test for assuring the reliability of a ceramic part may be from thirty to fifty and the price of test specimens reaches a large amount, especially for spacecraft and aircraft. Under these circumstances, if the same pre-

cision of the estimator could be obtained by using a smaller number of test specimens than before, it is more preferable. This paper discusses the effectiveness of using both fracture stress and fracture location to decrease the number of test specimens to achieve the same precision of the Weibull estimator on a bending load test.

2. Precision of Weibull estimator using both fracture stress and fracture location

According to Oh and Finnie's theory [2] modified by Matsuo and Kitakami [5, 6], the probability of a body being fractured by the l -th cause of fracture with reference stress range $(\sigma, \sigma + d\sigma)$ at a location $(\xi, \xi + d\xi)$ within an area A_1 is given by

$$f_{A_1}(\sigma, \xi) d\xi d\sigma = \exp(-B_l) \frac{\partial}{\partial \sigma} (G_l) d\xi d\sigma, \quad (1)$$

where $f_{A_1}(\sigma, \xi)$ is a joint probability density function (j.p.d.f.) relating to fracture stress σ and fracture location ξ , and B_l is a risk of fracture relating to the l -th cause of fracture. Here reference stress σ is the level of stress caused in the body by an external load, ordinarily represented by the maximum stress in the body. If the uniaxial Weibull distribution is used for the fracture

stress σ , B_l and G_l are given by

$$B_l = \int_{\xi \in A_l} G_l d\xi, \quad (2)$$

$$G_l = \left(\frac{\sigma_\xi - \sigma_{u_l}}{\sigma_l} \right)^{m_l} Y(\sigma_\xi, \sigma_{u_l}) \left(\frac{\partial A_l}{\partial \xi} \right)$$

where σ_ξ is the maximum principal stress at location ξ in the body; m_l , σ_l and σ_{u_l} ($l = 1, 2, \dots, \Lambda$) are shape, scale, and location parameters of the Weibull distribution related to the l -th cause of fracture; $Y(\sigma_\xi, \sigma_{u_l})$ is a Heaviside step function defined by

$$Y(\sigma_\xi, \sigma_{u_l}) \equiv \begin{cases} 1, & \text{if } \sigma_\xi > \sigma_{u_l} \\ 0, & \text{if } \sigma_\xi \leq \sigma_{u_l}. \end{cases}$$

Thus, using the competing risk theory with independent risks, the probability density function $f_A(\sigma, \xi)$ involving n causes of fracture is expressed as [6],

$$f_A(\sigma, \xi) = \prod_{i=1}^n R_i(\sigma) \sum_{j=1}^n \lambda_j,$$

$$R_i(\sigma) = 1 - \int_0^\sigma \int_{\xi_i} f_{A_i}(\sigma, \xi) d\xi d\sigma, \quad (3)$$

$$\lambda_j = f_{A_j}(\sigma, \xi) / R_j(\sigma),$$

$$A = A_1 \oplus A_2 \oplus \dots \oplus A_n.$$

Here \int_{ξ_i} means the integration over the total domain of A_i , \oplus symbol indicates direct sum. Equation 3 is valid for arbitrary state of stress and arbitrary type of fracture origin. Using this equation, we can obtain not only the joint probability density for fracture stress and fracture location, but also the distribution function of fracture stress, fracture location and/or crack size of fracture origin as a marginal of Equation 3 (see [6]).

From the view point of the reliability of ceramic parts, shape parameter, m_1 , plays the most important roles among the three parameters appeared in the above equations. Then it is generally called a ‘‘Weibull parameter’’. This paper focuses on the estimation of this parameter.

In this article, internal cracks ($l = 1$) and surface cracks ($l = 2$) are considered as the causes of fracture. Applying (1) to a 3-point bending load test (see Fig. 1), the j.p.d.f.s of fracture stress and fracture location become [5, 6]

$$f_{A1}(\sigma, x, y) = 2bm_1\sigma^{m_1-1} \left\{ \frac{x(h-y)}{\sigma_1 hL} \right\}^{m_1}$$

$$\cdot \exp \left\{ -V_e \left(\frac{\sigma}{\sigma_1} \right)^{m_1} \right\}, \quad (4)$$

$$f_{A2}(\sigma, x) = 2bm_2\sigma^{m_2-1} \left(\frac{x}{\sigma_2 L} \right)^{m_2}$$

$$\cdot \exp \left\{ -A_e \left(\frac{\sigma}{\sigma_2} \right)^{m_2} \right\}, \quad (5)$$

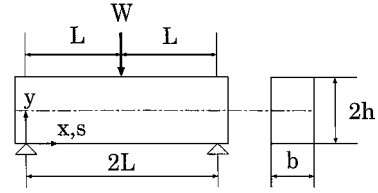


Figure 1 3-point bending load test and the sizes of specimen.

where

$$V_e = V_p \cdot V_{m_1}$$

$$V_p \equiv bhL, \quad V_{m_1} \equiv \frac{2}{(m_1 + 1)^2} \quad (6)$$

$$A_e = A_p \cdot A_{m_2}$$

$$A_p \equiv bL, \quad A_{m_2} \equiv \frac{2}{m_2 + 1}. \quad (7)$$

Since the Weibull parameter, m_1 and m_2 , are almost equal in many cases (e.g., [7]), we assume $m_1 = m_2 \equiv m$. Then, using the competing risks model, the observed likelihood becomes

$$L(m, \sigma_1, \sigma_2) = \frac{N!}{n_1!n_2!} \prod_{i=1}^{n_1} \left[2bm u_i^{m-1} \left\{ \frac{x_i(h-y_i)}{\sigma_1 hL} \right\}^m \right]$$

$$\times \exp \left\{ -V_e \left(\frac{u_i}{\sigma_1} \right)^m \right\} \times \exp \left\{ -A_e \left(\frac{u_i}{\sigma_2} \right)^m \right\}$$

$$\times \prod_{j=1}^{n_2} \left[2bm v_j^{m-1} \left(\frac{s_j}{\sigma_2 L} \right)^m \times \exp \left\{ -A_e \left(\frac{v_j}{\sigma_2} \right)^m \right\} \right]$$

$$\times \exp \left\{ -V_e \left(\frac{v_j}{\sigma_1} \right)^m \right\}, \quad (8)$$

where $\theta \equiv (m, \sigma_1, \sigma_2)'$, n_1 is the number of specimens fractured by the l -th cause. Let \hat{m} denote the maximum likelihood estimator (MLE) based on (8), and $AVar(\hat{m})$ be its asymptotic variance. From the result of [7], if K different design variables with the same height are considered, the optimum design is given by $K = 2$ with $N_1 = N_2 = N/2$, where N_k is the number of specimens in the k -th design variable (the k -th level). In this case, $AVar(\hat{m})$ becomes

$$AVar(\hat{m}) = \frac{1}{N} \left\{ \frac{p_1 + 1}{(m + 1)^2} + \frac{\pi^2}{6m^2} \right.$$

$$\left. + \frac{1}{4m^2} \log^2 \left(\frac{b_1 L_1}{b_2 L_2} \right) \right\}^{-1} \quad (9)$$

which attains its minimum value. p_1 is the probability of internal cracking and $b_k L_k$ represents the surface area of the k -th level ($k = 1, 2$). Throughout this paper, the heights of the specimens are assumed to be constant.

3. Precision of Weibull estimator using fracture stress or fracture location

If only the information regarding fracture stresses is available for estimating Weibull parameters, the

probability density functions (p.d.f.s) of the internal cracks and surface cracks are given by

$$\text{internal crack: } f_1(\sigma) = \frac{2bhL}{(m_1 + 1)^2} m_1 \frac{\sigma^{m_1-1}}{\sigma_1^{m_1}} \times \exp\left\{-Ve\left(\frac{\sigma}{\sigma_1}\right)^{m_1}\right\}, \quad (10)$$

$$\text{surface crack: } f_2(\sigma) = \frac{2bL}{m_2 + 1} m_2 \frac{\sigma^{m_2-1}}{\sigma_2^{m_2}} \times \left\{-Ae\left(\frac{\sigma}{\sigma_2}\right)^{m_2}\right\}, \quad (11)$$

respectively. Therefore, using the competing risks model the observed likelihood becomes

$$\begin{aligned} \tilde{L}(\theta) &= \frac{N!}{n_1!n_2!} \prod_{i=1}^{n_1} \left[\frac{2bhL}{(m+1)^2} m \frac{u_i^{m-1}}{\sigma_1^m} \right. \\ &\quad \times \exp\left\{-Ve\left(\frac{u_i}{\sigma_1}\right)^m\right\} \times \exp\left\{-Ae\left(\frac{u_i}{\sigma_2}\right)^m\right\} \left. \right] \\ &\quad \times \prod_{j=1}^{n_2} \left[\frac{2bL}{m+1} m \frac{v_j^{m-1}}{\sigma_2^m} \times \exp\left\{-Ae\left(\frac{v_j}{\sigma_2}\right)^m\right\} \right. \\ &\quad \times \exp\left\{-Ve\left(\frac{v_j}{\sigma_1}\right)^m\right\} \left. \right], \quad (12) \end{aligned}$$

where we set $m_1 = m_2 \equiv m$. Let \tilde{m} denote the MLE based on (12), and $AVar(\tilde{m})$ be its asymptotic variance. If the optimum design (two design variables and $N_1 = N_2 = N/2$: Proof is given in Appendix A.1) is applied, $AVar(\tilde{m})$ is given by

$$AVar(\tilde{m}) = \frac{m^2}{N} \left\{ \frac{\pi^2}{6} + \frac{1}{4} \log^2 \left(\frac{b_1 L_1}{b_2 L_2} \right) \right\}^{-1}. \quad (13)$$

If only the information on fracture locations is utilized, the p.d.f.s of the internal cracks and surface cracks are derived by integrating out σ of (4) and (5) as

$$\begin{aligned} \text{internal crack: } g_1(x, y) &= \int_{\sigma=0}^{\infty} f_{A1}(\sigma, x, y) d\sigma \\ &= \frac{(m_1 + 1)^2 \{x(h - y)\}^{m_1}}{(hL)^{m_1+1}}, \quad (14) \end{aligned}$$

$$\begin{aligned} \text{surface crack: } g_2(x) &= \int_{\sigma=0}^{\infty} f_{A2}(\sigma, x) d\sigma \\ &= \frac{(m_2 + 1)x^{m_2}}{L^{m_2+1}}, \quad (15) \end{aligned}$$

respectively. Putting $\lambda \equiv x/L$, $\mu \equiv y/h$, (14) and (15) become

$$q_1(\lambda, \mu) = (m_1 + 1)^2 \lambda^{m_1} (1 - \mu)^{m_1}, \quad (16)$$

$$q_2(\lambda) = (m_2 + 1) \lambda^{m_2}, \quad (17)$$

respectively. λ and μ represent the relative locations of fracture origins, and $q_1(\lambda, \mu)$ and $q_2(\lambda)$ are their p.d.f.s. They do not include variables that are related to the design variables. Therefore, even if the design variables are changed in experiments, there is no contribution by them to the precision of the estimators. The observed likelihood from N test specimens is given by

$$\begin{aligned} L^*(m) &= \frac{N!}{n_1!n_2!} \prod_{i=1}^{n_1} (m+1)^2 \lambda_i^m (1 - \mu_i)^m \\ &\quad \times \prod_{j=1}^{n_2} (m+1) \lambda_j^m, \quad (18) \end{aligned}$$

where we put $m_1 = m_2 \equiv m$. Let m^* denote the MLE based on (18), and $AVar(m^*)$ be its asymptotic variance. $AVar(m^*)$ is given by

$$AVar(m^*) = \frac{(m+1)^2}{N(p_1 + 1)}, \quad (19)$$

irrespective of the values of design variables (Proof is given in Appendix A.2).

In the following, we discuss the effectiveness of the utilization of both fracture stress and fracture location using $AVar(\hat{m})$, $AVar(\tilde{m})$ and $AVar(m^*)$. Table I represents $AVar(\hat{m})$, $AVar(\tilde{m})$ and $AVar(m^*)$ for $N = 10, 20, 30, 50, 100$, $b_1 L_1 / b_2 L_2 = 1, 2, 5, 10$, where we set $N_1 = N_2 = N/2$, $m = 17.0$, $\sigma_1 = 95.0$, $\sigma_2 = 109.95$ and $p_1 = p_2 = 0.5$.

From the table, the precision of the estimator \hat{m} measured by $AVar(\hat{m})$ becomes about two times better than that of $AVar(\tilde{m})$. This means that the number of test specimens need only one-half to achieve the same

TABLE I Comparison of the precisions of the estimators \hat{m} , \tilde{m} and m^* using their asymptotic variances

N	Number of design variables	$b_1 L_1 / b_2 L_2$	$AVar(\hat{m})$	$AVar(\tilde{m})$	$AVar(m^*)$
10	1	1.0	9.689	17.57	21.60
		2.0	9.314	16.37	
		5.0	7.960	12.61	
20	1	1.0	6.708	9.729	10.80
		2.0	4.844	8.785	
		5.0	4.657	8.187	
30	1	1.0	3.980	6.303	7.200
		2.0	3.354	4.865	
		5.0	3.230	5.856	
50	1	1.0	3.105	5.458	4.320
		2.0	2.653	4.202	
		5.0	2.236	3.243	
100	1	1.0	1.938	3.514	2.160
		2.0	1.863	3.275	
		5.0	1.592	2.521	
100	2	1.0	1.342	1.946	2.160
		2.0	0.969	1.757	
		5.0	0.931	1.637	
100	2	1.0	0.796	1.261	2.160
		2.0	0.796	1.261	
		5.0	0.671	0.973	

$N_1 = N_2 = N/2$, $p_1 = p_2 = 0.5$.

TABLE II Comparison of the precisions of \hat{m} , \tilde{m} and m^* for different m

N	m	$AVar(\hat{m})$	$AVar(\tilde{m})$	$AVar(m^*)$	$\frac{AVar(\tilde{m})}{AVar(\hat{m})}$	$\frac{AVar(m^*)}{AVar(\hat{m})}$
20	2.0	0.082	0.113	0.299	1.378	3.646
	5.0	0.445	0.708	1.198	1.591	2.692
	17.0	4.657	8.187	10.80	1.758	2.319

$$b_1L_1/b_2L_2 = 2.0, N_1 = N_2 = N/2, p_1 = p_2 = 0.5.$$

precision as in the case where only the information of fracture is used. In the table, $AVar(\hat{m})$ and $AVar(\tilde{m})$ are based on the optimum design. The larger b_1L_1/b_2L_2 , the better the precisions of \hat{m} and \tilde{m} . To the contrary, the precision of m^* is not affected by b_1L_1/b_2L_2 because $AVar(m^*)$ does not include these variables (the sizes of test specimens).

The following relation is held among $AVar(\hat{m})$, $AVar(\tilde{m})$ and $AVar(m^*)$ from (9), (13) and (19),

$$\frac{1}{AVar(\hat{m})} = \frac{1}{AVar(\tilde{m})} + \frac{1}{AVar(m^*)}. \quad (20)$$

Table II represents the comparison of the precisions of \hat{m} , \tilde{m} and m^* for different m . From the table, we know that the larger the value of m , the larger $AVar(\tilde{m})/AVar(\hat{m})$. That is, the effect of the utilization of both fracture stress and fracture location becomes larger as m increases compared with the case where the only fracture stress is used. Also, we know that the number of samples that is necessary to achieve the same precision when only the fracture stress is used becomes 1/1.758 times as large as that obtained by using both fracture stress and fracture location in the case $m = 17.0$.

4. Determining the numbers and sizes of specimens to attain the required precision

It is important to determine the number of test specimens in order to attain the required precision of

an estimator. For this purpose, the asymptotic variances $AVar(\hat{m})$, $AVar(\tilde{m})$ and $AVar(m^*)$ are presented in Tables III–VII, for the several combinations of m (Weibull shape parameter), σ_2/σ_1 (the ratio of Weibull scale parameters), and b_1L_1/b_2L_2 (the ratio of surface areas of specimens) where we set the height of specimen, $h = 3.0$ mm. The combinations are as follows;

$$m = \{5.0, 10.0, 15.0, 20.0, 30.0\},$$

$$\sigma_2/\sigma_1 = \{0.9, 1.0, 1.1\},$$

$$b_1L_1/b_2L_2 = \{1.0, 2.0, 5.0, 10.0, 20.0\}.$$

Here we use the optimum design where two design variables being of equal height and an equal number of specimens on each level are applied. The values of tables represent $N \times AVar(\cdot)$. That is, $AVar(\cdot)$ is obtained by dividing the values in table by N (the total number of specimens). For example, if $h = 3.0$, $m = 10.0$, $b_1L_1/b_2L_2 = 20.0$ and $\sigma_2/\sigma_1 = 1.1$, then from Table IV, we get $N \times Var(\hat{m}) = 19.77$. Therefore, if $N = 30$, $AVar(\hat{m})$ becomes $19.77/30 = 0.659$. Then a 95% confidence interval of m is given by

$$\begin{aligned} \hat{m} \pm 1.96\sqrt{Var(\hat{m})} &= \hat{m} \pm 1.96 \cdot \sqrt{0.659} \\ &= \hat{m} \pm 1.591. \end{aligned} \quad (21)$$

To examine the effect of the total number of specimens, N , on the precision, Fig. 2 represents the changes of $AVar(\hat{m})$, $AVar(\tilde{m})$ and $AVar(m^*)$ with N , where we set $h = 3.0$, $m = 20$, $b_1L_1/b_2L_2 = 5$, $\sigma_2/\sigma_1 = 1.0$ and $N_1 = N_2 = N/2$. The changes are very large when N is smaller than 30. Fixing $N = 30$, Fig. 3 shows the effect of b_1L_1/b_2L_2 on $AVar(\hat{m})$, $AVar(\tilde{m})$ and $AVar(m^*)$. From the figure, we know that the effectiveness of adding the fracture location information to that of the fracture stress is large when b_1L_1/b_2L_2 is

TABLE III Asymptotic variances of \hat{m} , \tilde{m} , and m^* , and the effectiveness of the fracture stress and fracture location information ($m = 5.0$)

$\frac{b_1L_1}{b_2L_2}$	$\frac{\sigma_2}{\sigma_1} (p_1)$	$N \cdot AVar(\hat{m})$	$N \cdot AVar(\tilde{m})$	$N \cdot AVar(m^*)$	$\frac{AVar(\tilde{m})}{AVar(\hat{m})}$	$\frac{AVar(m^*)}{AVar(\hat{m})}$
1.0	0.9 (0.228)	10.01	15.20	29.32	1.518	2.929
	1.0 (0.333)	9.724	15.20	27.00	1.563	2.777
	1.1 (0.446)	9.437	15.20	24.90	1.610	2.638
2.0	0.9	9.550	14.16	29.32	1.483	3.070
	1.0	9.290	14.16	27.00	1.525	2.906
	1.1	9.028	14.16	24.90	1.569	2.758
5.0	0.9	7.949	10.91	29.32	1.372	3.688
	1.0	7.768	10.91	27.00	1.404	3.476
	1.1	7.583	10.91	24.90	1.438	3.283
10.0	0.9	6.539	8.416	29.32	1.287	4.483
	1.0	6.416	8.416	27.00	1.312	4.208
	1.1	6.290	8.416	24.90	1.338	3.958
20.0	0.9	5.273	6.429	29.32	1.219	5.560
	1.0	5.193	6.429	27.00	1.238	5.200
	1.1	5.110	6.429	24.90	1.258	4.872

$AVar(\cdot)$ is obtained by dividing the above values by N .

$h = 3.0$, $N_1 = N_2 = N/2$, p_1 in bracket value represents the probability of fracture caused by an internal crack.

TABLE IV Asymptotic variances of \hat{m} , \tilde{m} , and m^* , and the effectiveness of the fracture stress and fracture location information ($m = 10.0$)

$\frac{b_1 L_1}{b_2 L_2}$	$\frac{\sigma_2}{\sigma_1} (p_1)$	$N \cdot AVar(\hat{m})$	$N \cdot AVar(\tilde{m})$	$N \cdot AVar(m^*)$	$\frac{AVar(\tilde{m})}{AVar(\hat{m})}$	$\frac{AVar(m^*)}{AVar(\tilde{m})}$
1.0	0.9 (0.087)	39.32	60.79	111.3	1.546	2.831
	1.0 (0.214)	37.76	60.79	99.65	1.610	2.639
	1.1 (0.414)	35.54	60.79	85.55	1.711	2.407
2.0	0.9	37.55	56.66	111.3	1.509	2.965
	1.0	36.12	56.66	99.65	1.569	2.759
	1.1	34.08	56.66	85.55	1.662	2.510
5.0	0.9	31.34	43.62	111.3	1.392	3.552
	1.0	30.34	43.62	99.65	1.438	3.284
	1.1	28.89	43.62	85.55	1.510	2.961
10.0	0.9	25.85	33.67	111.3	1.302	4.307
	1.0	25.16	33.67	99.65	1.338	3.960
	1.1	24.16	33.67	85.55	1.393	3.541
20.0	0.9	20.89	25.72	111.3	1.231	5.329
	1.0	20.44	25.72	99.65	1.258	4.875
	1.1	19.77	25.72	85.55	1.301	4.327

$AVar(\cdot)$ is obtained by dividing the above values by N .

$h = 3.0, N_1 = N_2 = N/2, p_1$ in bracket value represents the probability of fracture caused by an internal crack.

TABLE V Asymptotic variances of \hat{m} , \tilde{m} , and m^* , and the effectiveness of the fracture stress and fracture location information ($m = 15.0$)

$\frac{b_1 L_1}{b_2 L_2}$	$\frac{\sigma_2}{\sigma_1} (p_1)$	$N \cdot AVar(\hat{m})$	$N \cdot AVar(\tilde{m})$	$N \cdot AVar(m^*)$	$\frac{AVar(\tilde{m})}{AVar(\hat{m})}$	$\frac{AVar(m^*)}{AVar(\tilde{m})}$
1.0	0.9 (0.037)	88.01	136.8	246.8	1.554	2.804
	1.0 (0.158)	84.50	136.8	221.1	1.619	2.616
	1.1 (0.439)	77.32	136.8	177.9	1.769	2.300
2.0	0.9	84.06	127.5	246.8	1.516	2.936
	1.0	80.86	127.5	221.1	1.577	2.734
	1.1	74.26	127.5	177.9	1.717	2.395
5.0	0.9	70.22	98.15	246.8	1.398	3.515
	1.0	67.97	98.15	221.1	1.444	3.253
	1.1	63.25	98.15	177.9	1.552	2.812
10.0	0.9	57.96	75.75	246.8	1.307	4.259
	1.0	56.42	75.75	221.1	1.343	3.919
	1.1	53.12	75.75	177.9	1.426	3.348
20.0	0.9	46.87	57.86	246.8	1.234	5.266
	1.0	45.86	57.86	221.1	1.262	4.821
	1.1	43.66	57.86	177.9	1.325	4.074

$AVar(\cdot)$ is obtained by dividing the above values by N .

$h = 3.0, N_1 = N_2 = N/2, p_1$ in bracket value represents the probability of fracture caused by an internal crack.

TABLE VI Asymptotic variances of \hat{m} , \tilde{m} , and m^* , and the effectiveness of the fracture stress and fracture location information ($m = 20.0$)

$\frac{b_1 L_1}{b_2 L_2}$	$\frac{\sigma_2}{\sigma_1} (p_1)$	$N \cdot AVar(\hat{m})$	$N \cdot AVar(\tilde{m})$	$N \cdot AVar(m^*)$	$\frac{AVar(\tilde{m})}{AVar(\hat{m})}$	$\frac{AVar(m^*)}{AVar(\tilde{m})}$
1.0	0.9 (0.017)	155.8	243.2	433.6	1.561	2.783
	1.0 (0.125)	150.1	243.2	392.0	1.620	2.612
	1.1 (0.490)	133.5	243.2	296.0	1.822	2.217
2.0	0.9	148.8	226.6	433.6	1.523	2.913
	1.0	143.6	226.6	392.0	1.578	2.730
	1.1	128.3	226.6	296.0	1.766	2.306
5.0	0.9	124.4	174.5	433.6	1.402	3.485
	1.0	120.7	174.5	392.0	1.445	3.247
	1.1	109.8	174.5	296.0	1.590	2.696
10.0	0.9	102.8	134.7	433.6	1.311	4.220
	1.0	100.2	134.7	392.0	1.344	3.911
	1.1	92.55	134.7	296.0	1.455	3.198
20.0	0.9	83.14	102.9	433.6	1.237	5.215
	1.0	81.48	102.9	392.0	1.262	4.811
	1.1	76.34	102.9	296.0	1.348	3.877

$AVar(\cdot)$ is obtained by dividing the above values by N .

$h = 3.0, N_1 = N_2 = N/2, p_1$ in bracket value represents the probability of fracture caused by an internal crack.

TABLE VII Asymptotic variances of \widehat{m} , \widetilde{m} , and m^* , and the effectiveness of the fracture stress and fracture location information ($m = 30.0$)

$\frac{b_1 L_1}{b_2 L_2}$	$\frac{\sigma_2}{\sigma_1} (p_1)$	$N \cdot AVar(\widehat{m})$	$N \cdot AVar(\widetilde{m})$	$N \cdot AVar(m^*)$	$\frac{AVar(\widetilde{m})}{AVar(\widehat{m})}$	$\frac{AVar(m^*)}{AVar(\widehat{m})}$
1.0	0.9 (0.004)	348.1	547.1	957.1	1.572	2.749
	1.0 (0.088)	337.8	547.1	883.1	1.620	2.614
	1.1 (0.628)	283.9	547.1	590.3	1.927	2.079
2.0	0.9	332.7	509.9	957.1	1.533	2.877
	1.0	323.3	509.9	883.1	1.577	2.732
	1.1	273.6	509.9	590.3	1.864	2.158
5.0	0.9	278.4	392.6	957.1	1.410	3.438
	1.0	271.8	392.6	883.1	1.445	3.249
	1.1	235.8	392.6	590.3	1.665	2.504
10.0	0.9	230.1	303.0	957.1	1.317	4.159
	1.0	225.6	303.0	883.1	1.343	3.915
	1.1	200.2	303.0	590.3	1.513	2.948
20.0	0.9	186.4	231.5	957.1	1.242	5.135
	1.0	183.4	231.5	883.1	1.262	4.815
	1.1	166.3	231.5	590.3	1.392	3.550

$AVar(\cdot)$ is obtained by dividing the above values by N .

$h = 3.0$, $N_1 = N_2 = N/2$, p_1 in bracket value represents the probability of fracture caused by an internal crack.

small. From Equations 9, 13, and 19, we obtain

$$N \times AVar\left(\frac{\widehat{m}}{m}\right) = \left\{ \frac{p_1 + 1}{\left(1 + \frac{1}{m}\right)^2} + \frac{\pi^2}{6m^2} + \frac{1}{4m^2} \log^2\left(\frac{b_1 L_1}{b_2 L_2}\right) \right\}^{-1}, \quad (22)$$

$$N \times AVar\left(\frac{\widetilde{m}}{m}\right) = \left\{ \frac{\pi^2}{6} + \frac{1}{4} \log^2\left(\frac{b_1 L_1}{b_2 L_2}\right) \right\}^{-1}, \quad (23)$$

$$N \times AVar\left(\frac{m^*}{m}\right) = \left\{ \frac{p_1 + 1}{\left(1 + \frac{1}{m}\right)^2} \right\}^{-1}. \quad (24)$$

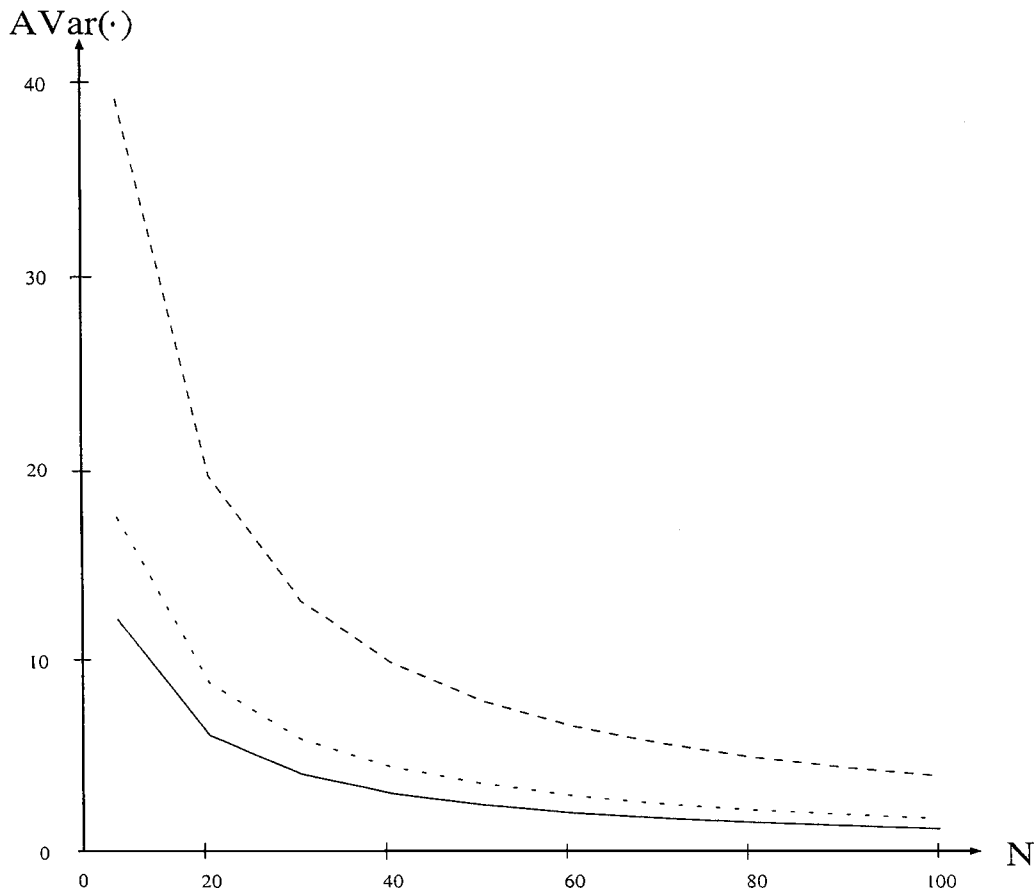


Figure 2 The effect of the total number of specimens, N , on the asymptotic variances of \widehat{m} , \widetilde{m} , and m^* ($h = 3$, $m = 20$, $b_1 L_1 / b_2 L_2 = 5$, $\sigma_2 / \sigma_1 = 1$ and $N_1 = N_2 = N/2$). $AVar(\widehat{m})$: the asymptotic variance when both fracture stress and fracture location are utilized. $AVar(\widetilde{m})$: the asymptotic variance when only the fracture stress is used. $AVar(m^*)$: the asymptotic variance when only the fracture location is used.

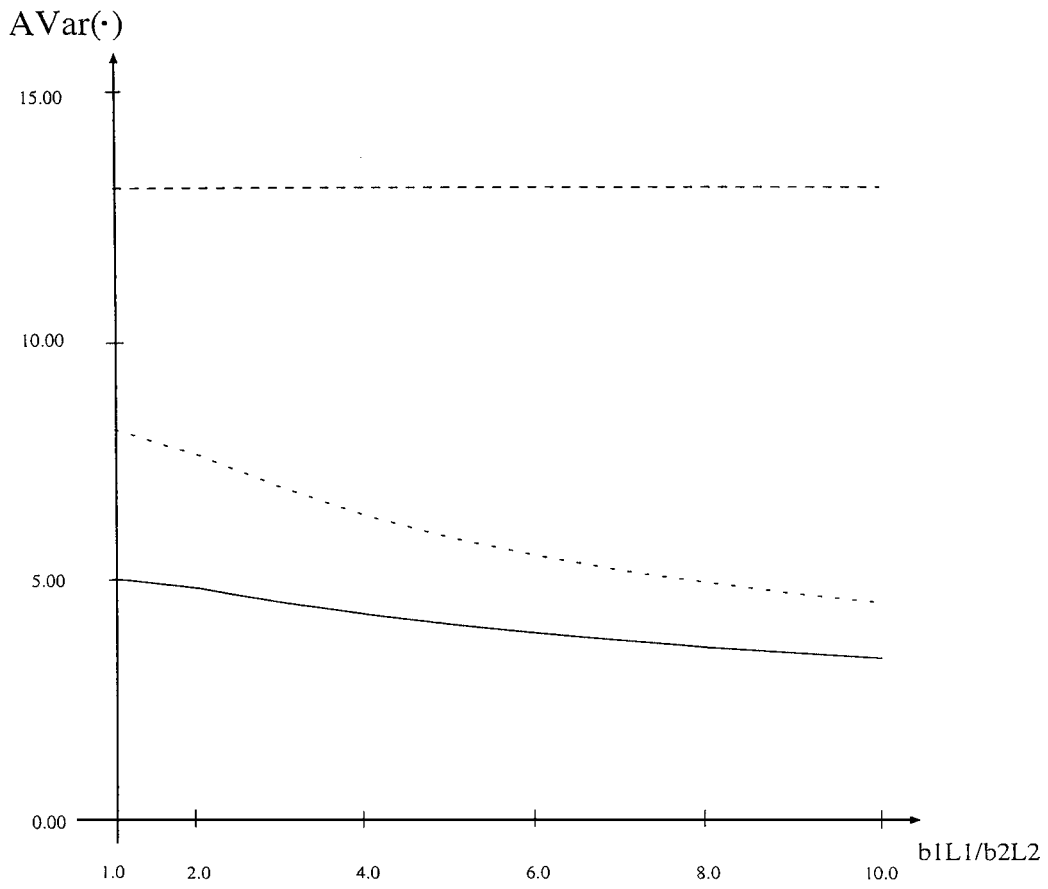


Figure 3 The effect of b_1L_1/b_2L_2 on the asymptotic variances of \hat{m} , \tilde{m} , and m^* ($h = 3$, $m = 20$, $\sigma_2/\sigma_1 = 1$ and $N_1 = N_2 = N/2 = 15$).

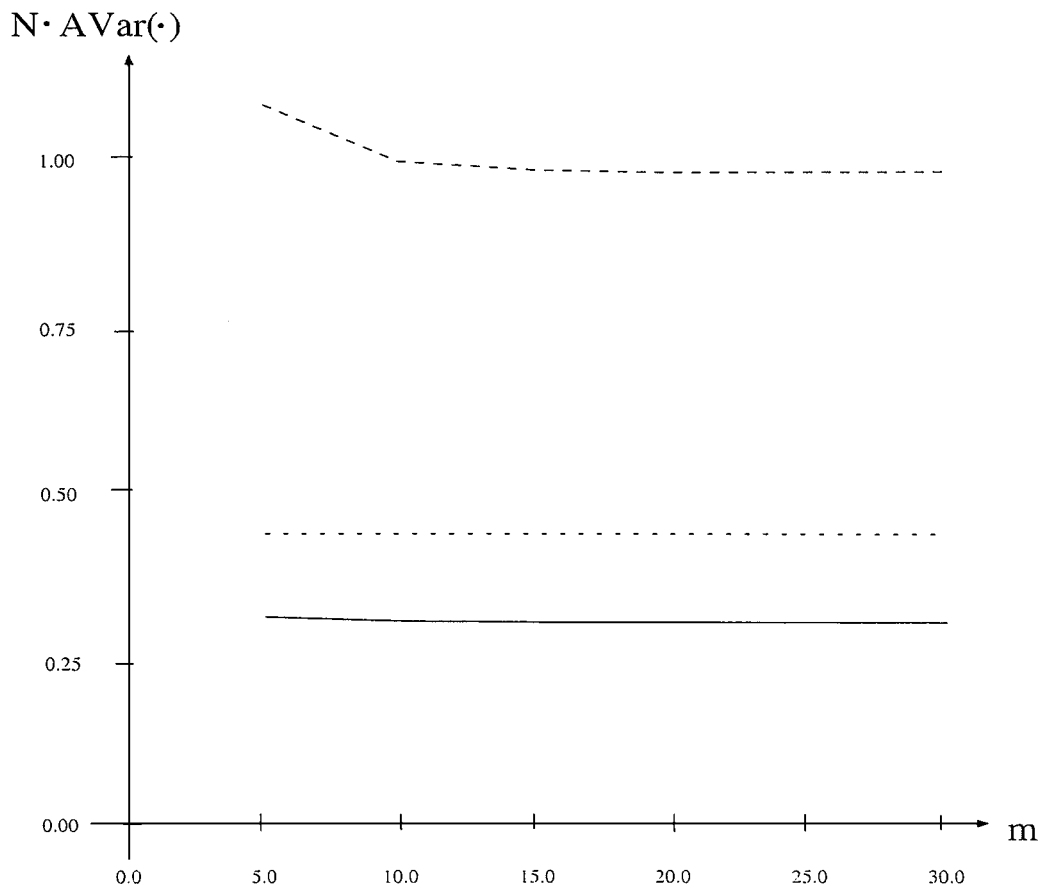


Figure 4 Effect of m on $AVar(\hat{m})$, $AVar(\tilde{m})$, and $AVar(m^*)$ ($h = 3$, $b_1L_1/b_2L_2 = 5$ and $\sigma_2/\sigma_1 = 1$).

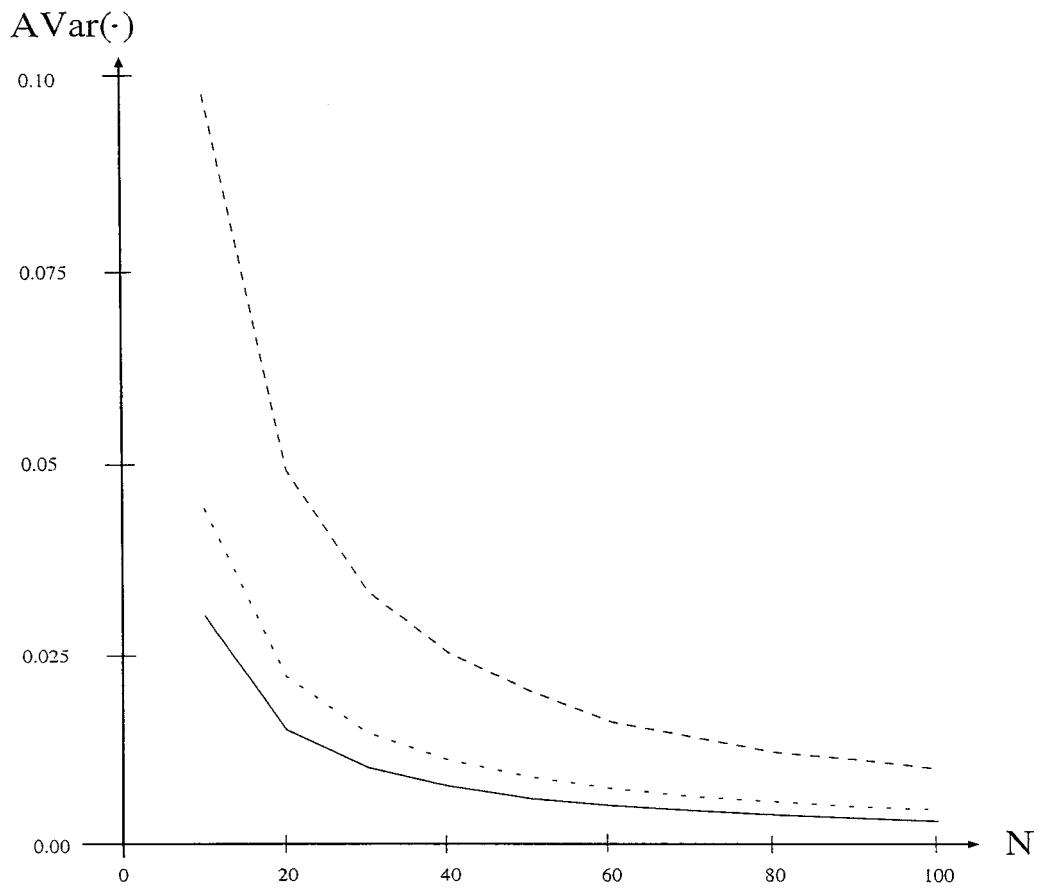


Figure 5 Effect of N on the asymptotic variances of $\frac{\hat{m}}{m}$, $\frac{\tilde{m}}{m}$, and $\frac{m^*}{m}$ ($h = 3, b_1L_1/b_2L_2 = 5, \sigma_2/\sigma_1 = 1, N_1 = N_2 = N/2$ and applicable for $m \geq 10$).

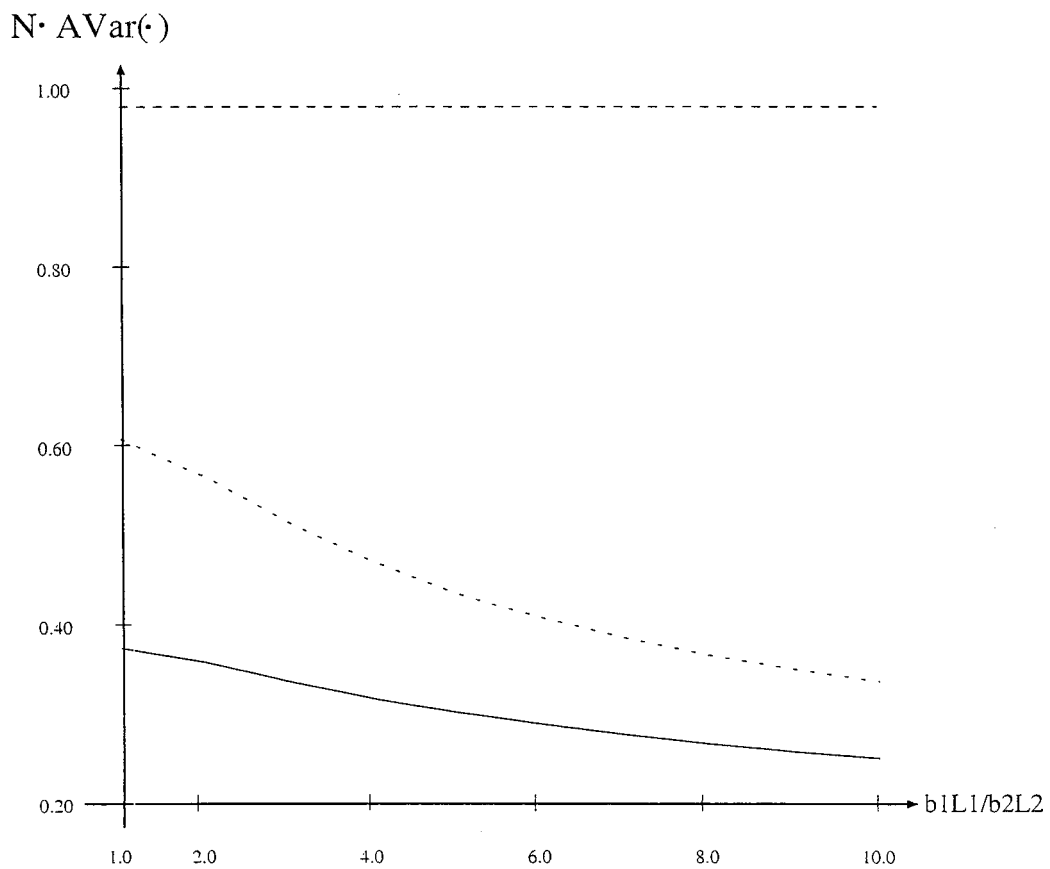


Figure 6 Effect of b_1L_1/b_2L_2 on the asymptotic variances of $\frac{\hat{m}}{m}$, $\frac{\tilde{m}}{m}$, and $\frac{m^*}{m}$ ($h = 3, \sigma_2/\sigma_1 = 1, N_1 = N_2 = N/2$ and applicable for $m \geq 10$).

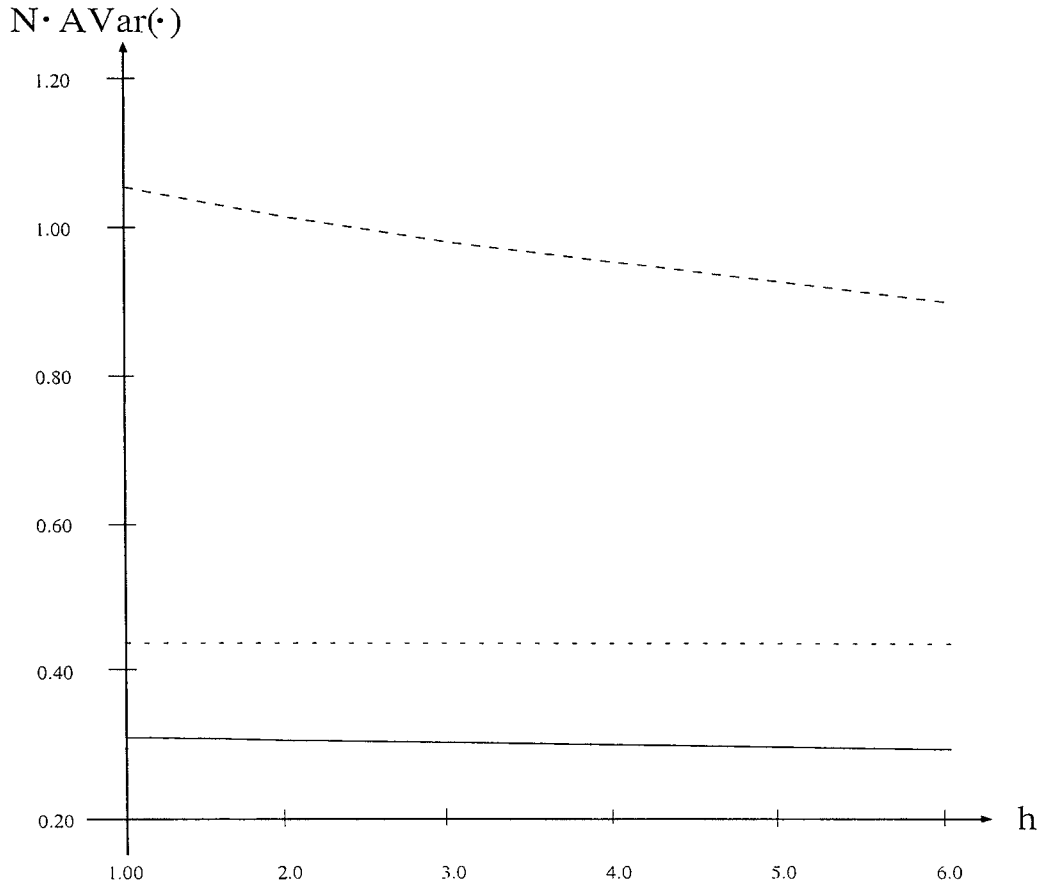


Figure 7 Effect of the height of a specimen h on the asymptotic variances of $\frac{\hat{m}}{m}$, $\frac{\tilde{m}}{m}$, and $\frac{m^*}{m}$ ($b_1L_1/b_2L_2 = 5$, $\sigma_2/\sigma_1 = 1$, $N_1 = N_2 = N/2$ and applicable for $m \geq 10$).

Therefore, the above quantities are not affected by m if m is large. Fig. 4 represents the effect of m on these quantities for a fixed h , b_1L_1/b_2L_2 and σ_2/σ_1 . From the figure, we know that if m is greater than 10, the asymptotic variances of \hat{m}/m , \tilde{m}/m and m^*/m become approximately constant, regardless of m . Therefore, in the following, we set $m = 20$ and examine the effect of N , b_1L_1/b_2L_2 and h on the variances. Fig. 5 shows the effect of N on the variances. Simi-

lar to Fig. 2, the effect of N is large when N is smaller than 30. Figs 6 and 7 show the effect of b_1L_1/b_2L_2 and h on the variances. The values of the vertical axis are multiplied by N . \hat{m} and \tilde{m} are not affected much by h , but m^* is largely affected. Hence, for fixed h and m , Table VIII shows the values of the asymptotic variances for $b_1L_1/b_2L_2 = 1, 2, 5, 10$ and 20 , and $\sigma_2/\sigma_1 = 0.9, 1.0$ and 1.1 . Table VIII corresponds to Table VI. From Tables III to VII, we know that the variance of \hat{m} becomes 1/1.5–1/1.9 times of that of \tilde{m} when $b_1L_1/b_2L_2 = 1$ or 2 . Therefore, the number of samples necessary to attain the same precision is given by 1/1.5–1/1.9 times compared with the case of using only fracture stresses.

TABLE VIII Asymptotic variances of $\frac{\hat{m}}{m}$, $\frac{\tilde{m}}{m}$, and $\frac{m^*}{m}$, and the effectiveness of the fracture stress and fracture location information

$\frac{b_1L_1}{b_2L_2}$	$\frac{\sigma_2}{\sigma_1}$ (p_1)	$N \cdot AVar(\frac{\hat{m}}{m})$	$N \cdot AVar(\frac{\tilde{m}}{m})$	$N \cdot AVar(\frac{m^*}{m})$
1.0	0.9 (0.017)	0.389	0.608	1.084
	1.0 (0.125)	0.375	0.608	0.980
	1.1 (0.490)	0.334	0.608	0.740
2.0	0.9	0.372	0.567	1.084
	1.0	0.359	0.567	0.980
	1.1	0.321	0.567	0.740
5.0	0.9	0.311	0.436	1.084
	1.0	0.302	0.436	0.980
	1.1	0.274	0.436	0.740
10.0	0.9	0.257	0.337	1.084
	1.0	0.251	0.337	0.980
	1.1	0.231	0.337	0.740
20.0	0.9	0.208	0.257	1.084
	1.0	0.204	0.257	0.980
	1.1	0.191	0.257	0.740

$AVar(\cdot)$ is obtained by dividing the above values by N . $h = 3.0$, $m = 20.0$, $N_1 = N_2 = N/2$, p_1 in bracket value represents the probability of fracture caused by an internal crack.

5. Conclusion

The effectiveness of adding the fracture location information to that of fracture stress on the Weibull parameter estimation under a 3-point bending load test is examined. The following results were obtained:

1. Adding the fracture location information, the precision of the estimate of the Weibull parameter under the optimal design becomes 1.5–1.9 times better than the case of using only fracture stresses. This means the number of samples required to attain the same precision becomes 1/1.5–1/1.9.

2. Tables and figures which give the information on the number of samples necessary to attain the required precision are given.

3. Asymptotic variances of \widehat{m}/m , \widetilde{m}/m and m^*/m were scarcely affected by the values of m when m is greater than 10.

A Appendix

A.1. Derivation of $AVar(\widetilde{m})$ and optimal design

In the case where only the fracture stress information is used, the Fisher information matrix is derived in the same way as [7]. If K design variables are applied, we get

$$AVar(\widetilde{m}) = m^2 \left(\frac{\pi^2}{6} N + \Delta_K \right)^{-1}, \quad (25)$$

where Δ_K is defined by

$$\begin{aligned} \Delta_K \equiv & \sum_{k=1}^K d_{k1} \log^2 \phi_k - \frac{\left(\sum_{k=1}^K d_{k1} \log \phi_k \right)^2}{\sum_{k=1}^K d_{k1}} \\ & + \sum_{k=1}^K d_{k2} \log^2 \phi_k - \frac{\left(\sum_{k=1}^K d_{k2} \log \phi_k \right)^2}{\sum_{k=1}^K d_{k2}}. \end{aligned} \quad (26)$$

In the case of $K = 2$ and the same heights, Δ_2 becomes

$$\Delta_2 = \left\{ -\frac{1}{N} \left(N_1 - \frac{N}{2} \right)^2 + \frac{N}{4} \right\} \log^2 \left(\frac{\phi_1}{\phi_2} \right). \quad (27)$$

and its maximum is given by

$$\frac{N}{4} \log^2 \left(\frac{b_1 L_1}{b_2 L_2} \right). \quad (28)$$

when $N_1 = N/2$. Therefore, we have

$$AVar(\widetilde{m}) = \frac{m^2}{N} \left\{ \frac{\pi^2}{6} + \frac{1}{4} \log^2 \left(\frac{b_1 L_1}{b_2 L_2} \right) \right\}^{-1}. \quad (29)$$

The optimality of $K = 2$ under some heights can be proven by the same approach as that reported in [2].

A.2. Derivation of $AVar(m^*)$

In the case where only the fracture location information is used, the second derivative of log likelihood based on (18) is given by

$$\frac{\partial^2}{\partial m^2} \log L^* = -\frac{1}{(m+1)^2} (2n_1 + n_2). \quad (30)$$

Therefore, the Fisher information matrix becomes

$$-E \left[\frac{\partial^2}{\partial m^2} \log L^* \right] = \frac{1}{(m+1)^2} (2E[n_1] + E[n_2]), \quad (31)$$

where $E[\cdot]$ represents the expectation of $[\cdot]$. Using $E[n_1] = N \cdot p_1$ and $E[n_2] = N \cdot p_2$, we get

$$AVar(m^*) = \frac{(m+1)^2}{N(p_1 + 1)}. \quad (32)$$

References

1. W. WEIBULL, *Ingeniors Ventenskaps Akademiens Handlingar* **151** (1939) 1.
2. H. L. OH and I. FINNIE, *Intern. J. Fract. Mech.* **6** (1970) 287.
3. S. AOKI and M. SAKATA, *Int. J. Fracture* **16** (1980) 459.
4. S. AOKI *et al.*, "Statistical Approach to Time-dependent Failure of Brittle Materials," *Int. J. Fracture* **21** (1983) 285.
5. Y. MATSUO and K. KITAKAMI, *J. Ceram. Soc. Jpn.* **93** (1985) 757 (in Japanese).
6. *Idem.*, "On the Statistical Theory of Fracture Location Combined with Competing Risk Theory," in *Fracture Mechanics of Ceramics*, Vol. 17, edited by R. C. Bradt *et al.* (Plenum Pub. Corp., 1986) p. 223.
7. K. SUZUKI, T. NAKAMOTO and Y. MATSUO, "Optimal Design for Estimating Weibull Shape Parameter Using Both Fracture Stress and Fracture Locations," Technical Report, University of Electro-Communications, Dept. of Communications and Systems Engineering, 2002, UEC-CAS-2002-01.

Received 21 February 2002
and accepted 21 August 2003